

Editorial Manager(tm) for Remote Sensing of Environment
Manuscript Draft

Manuscript Number: RSE-D-06-00658

Title: Surface movements in Bologna (Po Plain - Italy) detected by multitemporal DInSAR

Article Type: Full length article

Section/Category:

Keywords: SAR Interferometry; DInSAR SBAS; Subsidence; Water extraction; Active tectonics

Corresponding Author: Dr. Salvatore Stramondo, MD

Corresponding Author's Institution: Istituto nazionale di Geofisica e Vulcanologia

First Author: Salvatore Stramondo, MD

Order of Authors: Salvatore Stramondo, MD; Michele Saroli, Dr.; Cristiano Tolomei, Dr.; Marco Moro, Dr.;
Fawzi Doumaz, Dr.; Arianna Pesci, Dr.; Fabiana Loddo, Dr.; Paolo Baldi, Prof.; Enzo Boschi, Prof.

Manuscript Region of Origin:

Abstract:

Surface movements in Bologna (Po Plain - Italy) detected by multitemporal DInSAR

Stramondo S.^{1*}, Saroli M.^{1,2}, Tolomei C.¹, Moro M.¹, Doumaz F.¹, Pesci A.¹, Loddo F.¹, Baldi P.³, Boschi E.¹

¹ Istituto Nazionale di Geofisica e Vulcanologia – National Earthquake Center, Via di Vigna Murata 605, 00143 Rome-Italy E-mail: stramondo@ingv.it, tolomei@ingv.it, moro@ingv.it, doumaz@ingv.it, pesci@bo.ingv.it, loddo@bo.ingv.it, presidente@ingv.it

² University of Roma “La Sapienza”, Department of Sciences of the Earth, P. Aldo Moro 5, 00185-Roma (Italy); University of Cassino, Department of Civil Engineering, Via Di Biasio 43, 03043-Cassino

³ University of Bologna, Department of Physics, V.Berti Pichat, 8, 40127 Bologna (Italy), Tel: +39 051 2095011, E-mail: baldi@ibogfs.df.unibo.it,

* **Corresponding author: Salvatore Stramondo**, Istituto Nazionale di Geofisica e Vulcanologia – National Earthquake Center, Via di Vigna Murata 605, 00143 Rome-Italy Tel.: +39 06 51860521, Fax: +39 06 5041181

Abstract

We applied an advanced DInSAR technique, referred to as DInSAR-SBAS (Small BAseline Subset). This technique allows monitoring the temporal evolution of a deformation phenomenon, via the generation of mean deformation velocity maps and displacement time series from a data set of acquired SAR images. In particular, we have processed a dataset of SAR data acquired by the European Remote Sensing Satellite (ERS) sensors and compared the achieved results with optical levelling measurements, assumed as reference. The study area is the southeastern sector of the Po plain sedimentary basin, in particular the area of the Bologna town, historically affected by anthropogenic subsidence. We have provided an interpretation of the detected surface deformation by integrating such results with geological data. Former results from optical levelling referred to 1897 show 2-3 mm/year vertical movements. In the second half of the 20th century the subsidence rate reached 60 mm/year due to the

economic growth and the consequent human activity. The surface displacements detected by DInSAR SBAS from 1992 to 2000 are between 10 mm/year in the historical part of Bologna town, and up to 59 mm/year in the NE industrial and agricultural areas. The DInSAR detected deformation rate is in good agreement with levelling measurements relative to the 1992 and the late 1999 campaigns. The standard deviation of the difference between levelling data, projected onto the satellite Line Of Sight and DInSAR results is 2 mm/year. The explanation of soil movements by means of interferometric results, ground data and geological observations, allowed focusing on two hypotheses for possible causes: tectonic and anthropogenic subsidence.

1. Introduction

The city of Bologna is located at the Emilia Region Apennines foothill, along the southern boundary of the Po River sedimentary basin (Po Plain) (Fig. 1). As widely documented, the Po Plain is affected by subsidence due to the combination of a long term “natural” movement and the surface effects of “anthropogenic” activity (Carminati et al., 1988, Carminati & Di Donato, 1999; Bitelli et al., 2000; Marchetti, 2002; Carminati et al., 2003). Natural movements are the surface expression of different causes. In the literature, such causes are commonly referred to both tectonics (Cremonini & Ricci Lucchi, 1982; Bartolini et al., 1996), originated from the North Apennine thrust belt activity, sedimentary (loading and compaction) and post-glacial rebound (Carminati & Di Donato, 1999). These movements are not localized, but their influence is at a regional scale. According to previous papers dealing with natural subsidence it reaches a rate of 2.5 mm/year (Carminati & Di Donato., 1999; Carminati & Martinelli, 2002; Carminati et al., 2003). As far as anthropogenic causes are concerned, soil subsidence of the Po plain area is the surface effect of the overexploitation of the aquifers, as largely documented by technical reports (RER & ENI - Agip, 1998; RER, 2005; Rete IGM, 2004). Since the fifties, the urban area of Bologna rapidly expanded as a consequence of the industrial and agricultural development. Therefore compared with pre-industrial period, water extraction almost quadrupled during the second half of the 20th century. Indeed the comparison of levelling lines from the period 1897-1957 indicate subsidence rates of about 2-3 mm/year. In contrast, from 1957 to 2001 the average subsidence increased at 40-50 mm/year, and some benchmarks detected subsidence rates up to 60 mm/year in the northern suburbs of Bologna (Rete IGM, 2004). These subsidence rates in the Bologna city area are also confirmed by some GPS and gravimetric

measurements (Richter et al., 2003). We studied the temporal evolution of the surface deformation phenomenon by applying a multitemporal Differential Interferometry Synthetic Aperture Radar (DInSAR) technique known as Small BAseline Subset (DInSAR SBAS) (Berardino et al., 2002). The paper is organized as follows: first, an overview of the study area and its geological characteristics. The following sections concern a brief rationale of the DInSAR SBAS technique, the obtained results and the comparison with levelling measurements in the area of the Bologna city area. The further section is dedicated to the discussion, summarizing the main findings of this study. The last section is for some brief conclusive considerations.

2. Geological setting

The investigated area is in the Po Plain, bordered to the South by the Northern Apennines. The geological setting can be considered as the result of a foreland basin evolution process (Doglioni, 1993; Mariotti & Doglioni, 2000; Pieri & Groppi, 1981, Pieri, 1983; Royden, 1988) (Fig. 1) lying on the northern end-member of the Adriatic-Apulia block. From the Piemonte to the Adriatic, the large adjacent arcs enfold the plain Apennine structures, outlining the front of the buried Apennines chain (Boccaletti et al., 1985; Castellarin et al., 1985). Outside this was the Regional monoclinial (pede-Alpine monoclinial) (profile SSW-NNE in Fig. 1), a large and relatively undeformed structural element, foreland of the Pliocene Northern Apennines. In such context the Po Plain can be considered syntectonic sedimentary wedge (Cremonini & Ricci Lucchi, 1982) forming the infill of the Pliocene-Pleistocene Apenninic foredeep, a basin that was bounded by main belts (Apennines to the South Alps to the North) showing opposite polarity of tectonic transport (Apennines to the North, Alps to the South). It attains a total thickness

in excess of 4000 m; the Quaternary deposits are about 1000-2500 m thick (Pieri and Groppi, 1981). A major structural boundary between uplifting and subsiding crust occurs along the Southern margin of the Po Plain, the Pedè-Apenninic Thrust Front (PTF of Boccaletti et al., 1985; Amorosi et al., 1996) (Fig. 1, 2 and 3). This major structural element was also repeatedly active during the Pleistocene, as documented by a 600-700 m vertical offset Quaternary marine succession (Amorosi et al., 1996; Boccaletti et al., 2004; Castellarin et al., 1985). The compressive front Pedè-Apenninic Thrust Front of Northern Apennines does not correspond to the morphologic boundary between the mountain chain and the plain while it is possible to recognize this arched kind of limit in the Emilian and Ferraresi folds (Bartolini et al., 1996; Pieri & Groppi, 1981; Pieri, 1983). The evolution of this basin is due to the activation of the thrusts and to the re-activation of the preexisting thrusts (Boccaletti et al., 1985; Boccaletti & Sani, 1998; Boccaletti et al., 2004; Frepoli & Amato, 1997; Mariotti & Doglioni, 2000; Montone et al., 2004; Pieri & Groppi, 1981; Selvaggi & Amato, 1992). In this geological context, the Northern Apennine sector can be considered a thrust belt composed by tectonic units referred to “Ligure and Tosco-Umbro-Marchigiano domains” (CNR, 1992). On the contrary, the plain links the external portion of the Upper Miocene - Early Pliocene structured chain and the padano-adriatico sector. Here, the buried deformations are mainly referred to the Upper Pliocene-Quaternary, and some of the frontal thrusts are considered still active as well (Boccaletti et al., 1985; RER & ENI - Agip, 1998; Amorosi et al., 1996; Boccaletti et al., 2004). The edge of the relief and the alluvial plain beyond reflect a deep structural and geotectonic difference: the first one represents a raising zone, the second one a subsiding area (Pieri & Russo, 1977; Arca & Beretta, 1985; Bartolini et al., 1996; Folloni et al., 1996; D’Anastasio et al., 2006). In fact, as reported in the “Structural Model

of Regione Emilia-Romagna”, in the “Geological Map of the Po Plain”, in the “Seismotectonic Map of the Regione Emilia-Romagna” and in previous papers (Boccaletti et al., 2004), active compressive discontinuities are present (Fig. 2 and 3), parallel to the pre-Apennine edge, and are composed of Ligurian rocks and Imola sand deposits (Messinian-Middle Pleistocene). The same units are deeply depressed, and are also affected by an E-W trending fault system, coincident with the edge of the Sabbiano relief. The active Sabbiano anticline shows growth rates coherent with the effective tectonic activity of the “*thrust pede-appenninico*” (Amorosi et al., 1996), strongly constraining the erosional-depositional system (Bartolini et al., 1996). The same geological setting can be recognized in the alluvial plain, characterized by thick and recent alluvial sediments covering the orogene (“buried Apennine”) (CNR, 1992). This latter is represented by the Plio-Quaternary buried thrusts (see Fig. 2 and 3).

Geomorphologically we can recognize two distinct areas: the Apennines foothills and the lowlands in front. The deposits at the foot of the Sabbiano anticline have been affected by tectonic and lithostatic compaction (Elmi et al., 1984; Balestri & Villani, 1991). These folds are partially buried and hidden by Quaternary sediments. However, the Quaternary covering (Reno and Savena fan) of the lowlands, consists of recent and normal consolidated deposits. The aquifer is contained in the Plio-Quaternary marine and continental deposits. They fill the peristructural Padano basin originated by the Northern Apennine horogenic process. The RER & ENI - Agip (1998) and RER (2005) reports, highlights the presence of a multilayer and non continuous aquifer characterized by three hydrostratigraphic units (shallower Aquifer Group A, intermediate Aquifer Group B, deeper Aquifer Group C). Aquifer Group A (free watertable) is composed by alluvial deposits and the “Borgo Panigale Unit” (alluvial deposits and sands). Aquifer Group B is

a semi-confined aquifer composed by sand-clay alluvial deposits. Aquifer Group C is a confined aquifer (aquitard) consisting in tectonically deformed-marine deposits in the lower part and overconsolidated “Imola Sands and Yellow Sands” (Boccaletti et al., 2004; Elmi et al., 1984; RER & ENI – Agip, 1998; RER, 2005). As far as the Aquifer Group A and B are concerned they are not present close to the Sabbiano anticline (Boccaletti et al., 2004; Elmi et al., 1984; RER & ENI – Agip, 1998).

3. DInSAR SBAS: key issues

Space-based differential synthetic aperture radar interferometry has been widely applied to a single deformation episode (Gabriel et al., 1989; Massonet et al., 1993; Stramondo et al., 1999). The scientific interest recently moved towards the analysis of the temporal evolution of a deformation process by exploiting the phase difference of SAR image pairs. To follow the monitored deformation several approaches have been developed (Crosetto et al., 2005; Ferretti et al., 2001; Hooper et al., 2004; Mora et al., 2003; Usai et al., 2003; Werner et al., 2003). An effective way relies on computing a sequence of DInSAR interferograms, whose data pairs have a short separation between orbits (baseline) to reduce spatial decorrelation and topographic errors (Berardino et al., 2002). In this paper we apply the multitemporal DInSAR technique referred to as SBAS (Berardino et al., 2002). This approach implements the combination of a set of multilook DInSAR interferograms, thus leading to the generation of mean deformation velocity maps and displacement time series. The image pairs are properly chosen to mitigate the decorrelation phenomena (Zebker & Villasenor, 1992) and to obtain as many as possible coherent pixels. To this aim an upper bound either to the spatial and to the temporal separation between orbits is applied. The block diagram in Fig. 4 (modified from Casu et

al., 2006) summarizes the key points of the SBAS algorithm. The available SAR data have been co-registered with respect to a reference “master image”, Orbit 10769, May 12th, 1997. Afterwards a set of multilook DInSAR interferograms has been computed, each one calibrated respect to a stable point, referred to as the SAR reference pixel (see Fig. 2 and 4). Let express the generic interferogram as follows:

$$\Delta\phi_{21} = \phi_2 - \phi_1 \approx \frac{4\pi}{\lambda}(\delta_2 - \delta_1) + \Delta\phi_{topo} + \Delta\phi_{atmo} + \Delta n \quad (1)$$

where λ is the transmitted central wavelength, ϕ_2 and ϕ_1 are the phase components of the images that generate the interferogram, δ_2 and δ_1 are the detected deformations at times t_2 and t_1 (referred to a time t_0 , with $\phi_0 = 0$) projected onto the Line Of Sight (LOS). Moreover the term $\Delta\phi_{topo}$ contains possible topographic artifacts due to the DEM (Digital Elevation Model) used to generate the interferogram, whilst $\Delta\phi_{atmo}$ is relative to the atmospheric phase artifacts due to possible inhomogeneities between the two acquisitions (Goldstein 1995). Finally, the term Δn accounts for the noise effects due to decorrelation phenomena (Zebker & Villasenor, 1992).

The SBAS approach first identifies the coherent pixels for each interferogram, characterized by small values of Δn (Casu et al., 2006). Furthermore the informations from the computed interferograms are combined to cancel out $\Delta\phi_{topo}$ and $\Delta\phi_{atmo}$ in eq. 1, thus providing an estimate of the deformation time series for each coherent pixel. A phase retrieval procedure (i.e. the phase unwrapping) is then applied to each DInSAR interferogram. The phase unwrapping on a sparse grid of coherent pixels is based on the algorithm presented in Costantini & Rosen (1999), improved with a region growing procedure to maximize the propagation to areas with relatively low coherence (Casu et

al., 2006). The SBAS approach generates a linear system of equations, one for each DInSAR interferograms, to be solved on a pixel by pixel basis. Therefore the Singular Value Decomposition (SVD) method is applied to carry out a minimum norm Least Square solution. At this step the provided estimate of the deformation time series may contain also undesired contributions, as atmospheric artifacts and orbital ramps. It has been observed that the atmospheric signal is correlated in space while poorly in time (Ferretti et al., 2000). Therefore a Low Pass (LP) filter in space followed by a High Pass (HP) filter in time, applied to the time series, provides an estimate of the atmospheric signal. Parallely, as orbital ramps behaves similarly in space and time, the spatial LP and temporal HP filtering also detect such effects caused by inaccuracies of the orbital informations. This latter filtering leads to generate the effective deformation time series (Casu et al., 2006).

4. DInSAR SBAS: application and results

The surface deformation in Bologna had been already studied by means of DInSAR (Strozzi et al., 2001). Two subsidence maps spanning the time intervals 1992-1993 and 1997-1998 were calculated. For both cases six SAR data acquired by the ERS1-ERS2 (ERS - European Remote Sensing) satellites were used and the interferogram stacking technique was applied. We applied the DInSAR SBAS technique to measure the soil deformations in Bologna city and in the surrounding area. The method allows to generate a mean deformation velocity map with millimetric accuracy, and a deformation time series for each investigated pixel (coherent pixel) (Berardino et al., 2002; Lanari et al., 2004). To our aim we selected 52 ERS1-ERS2 SAR images on descending pass (track 394, frame 2691) spanning April 24th, 1992 - December 13th, 1999. As stated in

the previous section, to mitigate decorrelation phenomena in the multilook DInSAR interferograms we assumed 200 m as the maximum spatial separation (baseline) while 1000 days is the maximum time span. Based on such constraints, we computed 80 multilook interferograms from the available SAR dataset. The topographic phase has been removed by using a 20-m pixel size, 10 m accuracy, DEM provided by the Italian Geographic and Military Institute (IGM). Moreover precise orbit state vectors for ERS satellites, calculated from Delft University, have been used to reduce orbital errors. The DInSAR products, i.e. the mean velocity map and the SAR time series, have been generated with a complex multilook operation (4 looks in range direction, 20 in azimuth) thus obtaining a pixel size of about 80x80m. The mean velocity map showing the soil movements of the coherent pixels projected onto the satellite LOS is in Fig. 2. The reference point is in a stable area some km south of Bologna, where the benchmarks measured zero deformation along the four levelling campaigns performed from 1983 to 1999. Concerning the SAR time series they have been computed for each coherent pixel to follow the temporal evolution of the deformation.

5. DInSAR and levelling data comparison

Surface deformation has been detected by two independent techniques, DInSAR-SBAS and optical levelling. The 511 benchmarks measured (Rete IGM, 2004) are densely distributed in Bologna and its surroundings (Fig. 5). To our goal we focused on the last two campaigns (1992 and late 1999) that almost completely overlap the SAR dataset temporal span. The DInSAR mean velocity map (Fig. 2 and 5) is characterized by a high density of coherent pixels in the Bologna city, whilst it gradually degrades outside. This can be explained accounting for the frequent surface changes due to agricultural

activities all around Bologna affecting the temporal correlation of the SAR signal. In contrast, inside the city the surface scenario remains almost stable over time. Besides we observe that the mean surface velocity increases northwards. The detected subsidence rates are 2-5 mm/year along the piedmont sector of the Apennine belt close to the anticline (Fig. 2 and 3), but it though increases up to 40-50 mm/year towards the Reno River (WNW) and the Savena River (ESE) (Fig. 2 and 3). In the southern portion of the ancient Bologna, the mean subsidence velocity pattern ranges from 2 to 6 mm/year. Towards the north suburban area, where industrial and agricultural activities lead to a larger exploitation of water resources, surface velocity reaches 40-50 mm/year, and, very locally, up to 59 mm/year. To validate DInSAR results we compared the mean velocity with the vertical displacement measurements available from the levelling network in correspondence with the benchmarks surrounded by coherent pixels. So we computed the standard deviation of the difference between SAR and levelling benchmarks projected onto the LOS, $\sigma = 2.0 \text{ mm/year}$. A subset of 38 randomly selected benchmarks and their average displacements are in Table 1. In a recent paper (Casu et al., 2006) authors investigated the performance of the SBAS approach. They carried out a quantitative assessment of the SBAS procedure performance by processing SAR data acquired by the ERS sensors and comparing the achieved results with geodetic measurements that are assumed as reference. The comparison between DInSAR SBAS mean velocity and levelling measurements presented in this paper is in agreement with Casu et al. (2006). Concerning the temporal evolution of the subsidence it can be followed by analyzing the DInSAR time series for coherent points close to, or coinciding with, levelling benchmarks. To this aim we have provided a selection of 8

SAR coherent points and the contiguous benchmark. For each point we have superimposed the LOS projected levelling measurements and the deformation time series. Along the investigated period the DInSAR time series point out a general trend not diverging from a linear behaviour (except for leveling FID 267 and 385) (see Fig. 2 and 6). Moreover to infer further considerations about the previous years we accounted for levelling campaigns in 1983 and 1987. Based on such data it appears a general slowdown of the mean deformation from 1992 campaign.

6. Discussion

The surface subsidence in the Bologna area is due either to natural and to anthropogenic causes. Natural subsidence is the result of sediment compression and loss of interstitial fluids produced by rising above loading, natural compaction and tectonics. Concerning anthropogenic causes, they can be identified in the hydrocarbon and groundwater extraction, producing sediment compaction. Moreover from the second half of the 20th century, the economical growth of the main cities and the corresponding rising of new building blocks and urban structures increased the lithostatic loading and the sediment compaction. The RER & ENI – Agip (1998) identifies a multiple water table aquifer including A, B and C Aquifer Groups. Aquifer Group A, the shallowest and the most affected by subsidence, is predominant in the study area. We compare the DInSAR mean velocity map with the isobaths of the Aquifer Group A (Fig. 2 and 3). It is possible to observe a general trend: in those areas where the surface velocity (i.e. the subsidence) is higher, the Aquifer Group A, mainly exploited by groundwater withdrawal, is thicker (Fig. 2 and 7). This correspondence suggests that the main cause of the SAR detected subsidence is water extraction from the shallowest

Aquifer Group C (aquitard, not affected by water extraction) allow assuming tectonic activity as the most reliable cause of this slow surface deformation. To enforce such hypothesis, seismological data point out that the hypocentral distribution from instrumental seismicity is mainly localized at depth south of the structure corresponding with the frontal thrust of the Apenninic chain (Fig. 7).

7. Conclusions

We investigated the surface deformations of Bologna city and its surroundings during 1992-2000 by means of the DInSAR SBAS technique and geological data. In previous papers the whole subsidence in and around the Bologna city area has been explained as the consequence of the intensive water extraction from the Aquifer Group A and B. We compared the DInSAR SBAS mean velocity map and the levelling measurements, i.e. our reference data, of 1992 and late 1999 campaigns, projected onto the SAR LOS. The standard deviation of the difference SAR/LOS levelling is about 2mm/y. The temporal evolution of the detected subsidence follows a pretty linear trend, as shown in SAR time series of selected points. However the levelling campaigns in 1983 and 1987 demonstrate a slowdown of surface deformation from 1992.

The geological analysis allows assuming that the larger amount of the detected subsidence (40-50 mm/year) is due to the abovementioned cause. As a matter of fact it takes place in the area of thicker deposits of the Po Plain, corresponding with the Aquifer Group A and B. Furthermore, as also highlighted by many authors (Amorosi et al., 1996; Arca and Beretta, 1985; Bartolini et al., 1996; Boccaletti et al., 1985; Boccaletti & Sani, 1998; Boccaletti et al., 2004; Carminati & Di Donato, 1999; Carminati & Di Donato, 2002; Pieri, 1983; Pieri & Groppi, 1981; Pieri & Russo, 1977), our results

confirm the existence of a natural, tectonic component of the displacement in the Apennine piedmont belt (Sabbiuno anticline) immediately close to the southern portion of Bologna. The detected amount of such displacement ranges 2-5 mm/year. The area close to the piedmont Sabbiuno anticline, coinciding with the active thrust, is also characterized by the absence of the Aquifer Group A and B. This element, together with the results of our analysis, is a further aspect enforcing the tectonic activity (interseismic) as the main cause for the movements observed in this area.

Acknowledgments:

We warmly thank Prof. Riccardo Caputo for the professional and valuable scientific advice. We thank also Dr. Giovanni Martinelli for the helpful discussions. A particular thank to Dr. Riccardo Lanari for his advises and basic suggestions concerning the SBAS technique. The SAR images used in this work were provided by European Space Agency (ESA) in the framework of the EO CAT1 2796 project.

References

- Amorosi, A., Farina, M., Severi, P., Preti, D., Caporale, L. & Di Dio, G. (1996). *Genetically related alluvial deposits across active fault zones: an example of alluvial fan-terrace correlation from the upper quaternari of the southern Po Basin, Italy*. Sedimentary Geology, 102, 275-295.
- Arca, S., and Beretta, G.,P. (1985). prima sintesigeodetico-geologica sui movimenti verticali del suolo nell'Italia Settentrionale (1897-1957). Boll. Geod. Sc. Affini 2, 125-156.

Balestri, M., and Villani, B. (1991). Study of the subsidence in the Bologna area. Proceedings of the Fourth International Symposium on land Subsidence, May 1991, IAHS Publ. n. 200.

Bartolini, C., Caputo, R., and Pieri, M. (1996). Pliocene-Quaternary sedimentation in the Northern Apennine Foredeep and related denudation. *Geological Magazine*, vol.133, no.3, pp.255-273.

Berardino, P., Fornaro, G., Lanari, R., & Sansosti, E. (2002). A new Algorithm for Surface Deformation Monitoring based on Small Baseline Differential SAR Interferograms. *IEEE Trans on Geosci. and Remote Sensing*, 40, 2375-2383.

Bitelli, G., Bonsignore, F., & Uguendoli, M. (2000). Levelling and GPS network to monitor round susidence in the Southern po valley. *J. Geodyn.*, 30, 355-369.

Boccaletti, M., Coli, M., Eva, C., Ferrari, G., Giglia, G., Lazzaretto, A., Merlanti, F., Nicolich, R., Papani, G., & Postpischl, D. (1985). *Considerations on the seismotectonics of the Northern Apennines*. *Tectonophysics*, 117, 7-38.

Boccaletti, M., & Sani, F. (1998). *Cover thrust reactivations related to internal basement involvement during Neogene-Quaternary evolution of the Northern Apennines*. *Tectonics*, 17, 112-130.

Boccaletti, M., Bonini, M., Corti, G., Gasperini, P., Martelli, L., Piccardi, L., P. Severi, P, & Vannucci, G. (2004). Carta sismotettonica della regione Emilia-Romagna. Scala 1:250.000. Note Illustrative, *Serv. Geol. Sismico e dei Suoli, Reg. Emilia Romagna*, SELCA-Firenze.

Carminati, E., Wortel, M.,J.,R., Spakman, W., & Sabadini, R., (1988). A new model for the opening of the western-central Mediterranean basins. *Geological ad geophysical*

constraints for a major role of slab detachment. *Earth and planetary Science Letters*, 1600, 651-654.

Carminati, E., & Di Donato, G. (1999). Separating natural and anthropogenic vertical movements in fast subsiding areas: the Po plain (N Italy) case. *Geophys. Res. Lett.*, **26**, 2291-2294.

Carminati, E., & Martinelli, G. (2002). Subsidence rates in the Po Plain, northern Italy: the relative impact of natural and anthropogenic causation. *Engineering Geology*, 66, 241-255.

Carminati, E., Doglioni, C., & Scrocca, D. (2003). Appennines subduction-related subsidence of Venice (Italy). *Geophys. Res. Lett.*, 30, 10.1029/2003GL017001.

Castellarin, A., Eva, C., Giglia, G., Vai, G.B., Rabbi, E., Pini, G.,A. & Crestana, G. (1985). Analisi strutturale del fronte appenninico padano. *G. Geol.*, 47, 47-75

Casu, F., Manzo, M., Lanari, R. (2006). A quantitative assessment of the SBAS algorithm performance for surface deformation retrieval from DInSAR data. *Remote Sensing of Environment* 102 195–210.

CNR (1992). Structural Model of Italy, 1:500,000. Prog. Fin. Geodin. S.P. 5, Quaderni de “La Ricerca Scientifica” n° 114, S.EL.CA., Firenze

Costantini, M., & Rosen, P. A. (1999). A generalized phase unwrapping approach for sparse data. *IGARSS'99 Proc.*, Hamburg (Germany) (pp. 267–269)

Cremonini, G., Ricci Lucchi, F. (eds) (1982). Guida alla geologia del margine appenninico-padano, Guide Geologiche Regionali, Società Geologica Italiana.

Aquifer Group A. However far from the Sabbiano anticline, whereas the thickness of Aquifer Group A is reduced whilst the DInSAR mean velocity remains high, such effect is the consequence of groundwater withdrawal affecting the Aquifer Group B (RER & ENI – Agip, 1998; RER, 2005). Concerning the natural causes, previous studies (Carminati et al., 1988; Carminati & Di Donato, 1999; Carminati & Martinelli, 2002; Carminati et al., 2003) supported the hypothesis that part of the subsidence is due to this latter, in particular to tectonics. The natural subsidence rate obtained from commercial data has been estimated up to 2.5 mm/year (Fig. 2 and 3) in the southern portion of the Po plain (Carminati & Di Donato, 1999). The study area is characterized by the recent activity of the Sabbiano anticline associated with a blind thrust (Fig. 2 and 3). Its activity is confirmed by morphometric indexes and by the presence of fault scarps in Holocene fan (Boccaletti et al., 2004). Moreover, geological evidence of this structure includes the compressive deformations of the Imola sands and of the Middle Pleistocene deposits near Bologna. In particular the Imola sands, the more external margin of the anticline in the southern portion of old Bologna, are bounded by the active thrust inside the city (Fig. 2, 3, 7). This tectonic structure partially affects the deposits of Aquifer Group C and the bedrock composed by the Ligurian rocks (Sabbiano anticline) (Fig. 3 and 7) which, therefore, result deformed. The surface trace of the outcropping active thrust is within the sector where DInSAR findings highlight surface movements ranging 2-5 mm/year (Fig. 3). Moreover the soil movement increases up to 5 mm/year very close to the surface expression of the thrust (Fig. 7). The absence of the Aquifer Group A and B (RER & ENI – Agip, 1998; RER, 2005), the contemporary presence of an active blind thrust (Boccaletti et al., 1985; Boccaletti et al., 2004; Pieri & Groppi, 1981; Pieri et al., 1983) and, key issue, the presence of overconsolidated deposits (Elmi et al., 1984) of

Crosetto, M., Crippa, B., & Biescas, E. (2005). Early detection and in-depth analysis of deformation phenomena by radar interferometry. *Engineering Geology*, 79(1–2), 81–91.

D'anastasio, E., De Martini, P., M., Selvaggi, G., Pantosti, D., Marchioni, A., Maseroli, R. (2006). Short-term vertical velocity field in the Apennines (Italy) revealed by geodetic levelling data. *Tectonophysics*, 418, 219-234.

Doglioni, C. (1993). Some remarks of the origin of foredeeps. *Tectonophysics*, 228, 1-20.

Elmi, C., Bergonzoni, A., Massa, T., Mantaletti, V., Bagattella, P.L., Ronchi, A. (1984). Il territorio di pianura del comune di Bologna: aspetti geologici e geotecnica. *Giornale di geologia*, sr. 3°, 46/2.

Ferretti, A., Prati, C. & Rocca, F. (2000). Non-linear subsidence rate estimation using permanent scatterers in differential SAR Interferometry. *IEEE Trans. Geosci. Remote Sensing*, 38, 5.

Ferretti, A., Prati, C., & Rocca, F. (2001). Permanent scatterers in SAR interferometry. *IEEE Trans. Geosci. Remote Sensing*, vol.39, pp.8-20, Jan. 2001.

Folloni G., Russo, P., & Radicioni, F. (1996). La subsidenza del territorio bolognese dal 1983 al 1993. *Inarcos*, 571, 400-413.

Frepoli, A., & Amato, A. (1997). Contemporaneous extension and compression in the northern Apennines from earthquakes fault-plane solutions. *Geophys. J. Int.*, 129, 368-388.

Gabriel, A., Goldstein, R., & Zebker, H. (1989). Mapping small elevation changes over large areas: Differential radar interferometry. *J. Geophys. Res.*, **94**, 9183–9191.

Goldstein, R.M. (1995). Atmospheric limitations to repeat-track radar interferometry. *Geophysical Research Letters*, 22, 2517-2520.

Hooper, A., Zebker, H., Segall, P., & Kampes, B. (2004). A new method for measuring deformation on volcanoes and other natural terrains using InSAR persistent scatterers. *Geophysical Research Letters*, 31, L23611. doi:10.1029/2004GL021737

Lanari, R. , Mora, O., Manunta, M., Mallorqui, J., Berardino, P., & Sansosti, E. (2004). A Small Baseline Approach for Investigating Deformations on Full Resolution Differential SAR Interferograms. *IEEE Transactions on Geosci. and Remote Sensing*, **42**, 1377-1386.

Marchetti, M. (2002). Enviromental changes in the Central Po plain (Northern Italy) due to fluvial modifications and anthropogenic activities. *Geomorphology*, **44**, 361-373.

Mariotti, G., & Dogliosi, C. (2000). The dip of the foreland monocline in the Alps and Apennines. *Earth and Planetary Science Letters*, 181, 191-202.

Massonet, D., Rossi, M., Carmona, C., Adragna, F., Peltzer, G., Feigl, K., & Rte, T. (1993). The displacement field of the Landers earthquake mapped by radar interferometry. *Nature*, **364**, 138-142.

Montone, P., Mariucci, M., T., Pondrelli, S., Amato, A. (2004). An improved stress map for Italy and sourrounding regions (central Mediterranean). *J. Geoph. Res.*, **109**, 1-22.

Mora, O., Mallorquí, J. J., & Broquetas, A. (2003). Linear and nonlinear terrain deformation maps from a reduced set of interferometric SAR images. *IEEE on Transaction Geoscience and Remote Sensing*, 41, 2243–2253.

Pieri, M. (1983). Three seismic profiles through the Po Plain. In: Seismic Expression of Structural Styles. A Picture and Work Atlas (A.W. Bally, ed). Am. Assoc. Pet. Geol. Stud. Geol., 15, 3.4.1/8–3.4.1/26.

Pieri, M., & Groppi, G. (1981). Subsurface geological structure of the Po Plain (Italy). *C.N.R., Prog. Fin. Geodinamica*, **414**, 1-13.

Pieri, M., & Russo, P. (1977). Studio del fenomeno di abbassamento del suolo in atto nella zona di Bologna. *Bollettino di Geodesia e Scienze Affini*, 3, 365-388

RER & ENI - Agip (1998). Riserve idriche sotterranee della Regione Emilia-Romagna. *Regione Emilia-Romagna - ENI divisione Agip.*, S.EL.CA., Firenze, 120.

RER (2005). Le caratteristiche degli acquiferi della regione Emilia Romagna. Report 2003. ARPA – Agenzia Regionale Prevenzione Ambiente dell'Emilia Romagna.

Rete IGM, Rete Grande Bologna, Rete Raffinamento Bologna, Rete Autorità di Bacino del Reno, Rete Provinciale, Rete Regionale, 2004. *Comune di Bologna*.

Richter, B., Zerbini, S., Lago, L., Romagnoli, C., Simon, D. (2003). Long-Term Crustal Deformation Monitored By Gravity And Space Techniques At Medicina. *Geophysical Research Abstracts*, Vol. 5, 09162, 2003, European Geophysical Society.

Royden, L.E. (1988). Flexural behaviour of the continental lithosphere in Italy: constraints imposed by gravity and deflection data. *J. Geophys. Res.*, 93, 7747–7766.

Selvaggi, G. & Amato, A. (1992). *Subcrustal earthquakes in the Northern Apennines (Italy): evidence for a still active Subduction?*. *Geophysical Research Letters*, 19, 2127-2130.

Stramondo, S., Tesauro, M., Briole, P., Sansosti, E., Salvi, S., Lanari, R., Anzidei, M., Baldi, P., Fornaro, G., Avallone, A., Buongiorno, M.F., Franceschetti, G., Boschi, E. (1999): *The September 26, 1997 Colfiorito, Italy, earthquakes: modeled coseismic surface displacement from SAR interferometry and GPS*. Geophys. Res. Lett., 26 (7), 883-886.

Strozzi, T., Wegmüller, U., Tosi, L., Bitelli, G., & Spreckels, V. (2001). Land Subsidence Monitoring with Differential SAR Interferometry. PE&RS (Photogrammetric Engineering & Remote Sensing), Vol. 67, Nr. 11, pp. 1261-1270.

Usai, S. (2003). A least squares database approach for SAR interferometric data. IEEE Transactions on Geoscience and Remote Sensing, 41(4), 753–760.

Werner, C., Wegmuller, U., Strozzi, T., & Wiesmann, A. (2003). Interferometric point target analysis for deformation mapping. Proceedings of IGARSS '03, vol. 7. (pp. 4362–4364).

Zebker, H.A., & Villasenor, J. (1992). Decorrelation in interferometric radar echoes. IEEE Transactions on Geoscience and Remote Sensing, 30, 950-959.

Captions

Fig. 1. Seismotectonic map of the study area. The instrumental earthquakes recorded by the Istituto Nazionale di Geofisica between 1981 and 2002 are in yellow: circles ($M < 4$), squares ($4 < M < 5$), stars ($M > 5$). Historical events are indicated by red squares (Gruppo di Lavoro CPTI, 1999). White crosses represent the orientation of horizontal stress (S_h min) deduced from breakout and focal mechanism analysis (Montone et al., 2004). White line is the direction of Profile 1 in Fig. 2, 3 and 6. PTF: Pede-Apenninic Thrust Front (of Boccaletti et al., 1985; Amorosi et al., 1996)

Fig. 2. Surface DInSAR mean deformation velocity map spanning 1992-2000. The time series relative to levelling benchmarks along Profile 1 (white circles) are in Fig. 6. The reference point of the DInSAR velocity is also shown (red circle).

Fig. 3. Schematic geological map of the study area. The 2-5 mm/year DInSAR SBAS mean velocities (yellow), selected from velocity map in Fig.2, are also shown.

Fig. 4. Block diagram of the DInSAR SBAS rationale (modified from Casu et al., 2006).

Fig. 5. Surface mean velocity map as in Fig.2 and levelling benchmarks (black dots, fuchsia and white circles). Fuchsia and white circles are the 38 randomly selected benchmarks in Table 1. Besides the 8 white ones are the levelling benchmarks in Fig. 6 and n.385, 398, 487, 340, 250 are also those in Fig.1 and 2. The reference point of the DInSAR mean velocity is also shown (red circle).

Fig. 6. (a,b,c,d,e,f,g,h) Comparison between the DInSAR SBAS deformation time series of coherent points (in blue) and the corresponding levelling measurements (in fuchsia) projected on the SAR LOS for the 8 white benchmarks in Fig. 5. Levelling campaigns are in 1983, 1987, 1992 and late 1999. R^2 is the correlation index between the time series and the linear trending line.

Fig. 7. Schematic data correlation between SAR surface velocity, thickness of aquifers and simplified geological and hydrostratigraphic cross section along Profile 1 (see Fig. 1, 2 and 3).

Table 1. Comparison between levelling measurements of the 38 selected benchmarks (fuchsia circles) in Fig. 5 and the DInSAR SBAS mean velocity deformation at coherent points. Levelling data relative to the 1992 and 1999 are also projected on the SAR LOS.

Table1

FID	Levelling 1992-1999 (mm/y)	Levelling in SAR LOS (mm/y)	DInSAR surface velocity (mm/y)	Difference (mm/y)
499	0	0.0	0.3	-0.3
506	-1	-0.9	0.2	0.7
0	0	0.0	0.1	-0.1
266	7	6.4	4.5	1.9
157	14	12.9	14.0	-1.1
19	16	14.7	11.6	3.1
440	0	0.0	0.0	0.0
149	19	17.5	18.0	-0.5
456	12	11.0	7.0	4.0
381	15	13.8	8.3	5.5
328	23	21.2	18.5	2.7
341	30	27.6	26.6	1.0
332	24	22.1	17.3	4.8
338	36	33.1	31.4	1.8
296	37	34.1	34.6	-0.5
318	41	37.7	32.2	5.5
305	16	14.7	12.6	2.1
216	22	20.3	22.6	-2.3
159	18	16.6	15.9	0.7
219	45	41.4	37.5	3.9
479	30	27.6	23.2	4.4
144	9	8.3	7.0	1.3
153	38	35.0	33.0	2.0
343	11	10.1	9.7	0.4
96	1	0.9	0.0	0.9
250	31	28.5	25.8	2.7
267	0	0.0	0.4	-0.4
340	32	29.5	26.0	3.5
480	31	28.5	27.0	1.5
398	8	7.4	3.1	4.3
385	1	0.9	0.3	0.6
487	34	31.3	30.0	1.3
396	6	5.5	-4.4	1.1
278	25	23	18	5
275	7	6.4	7	-0.6
232	39	35.9	31	4.9
473	33	30.4	27	3.4
242	37	34	29	5

Figure1

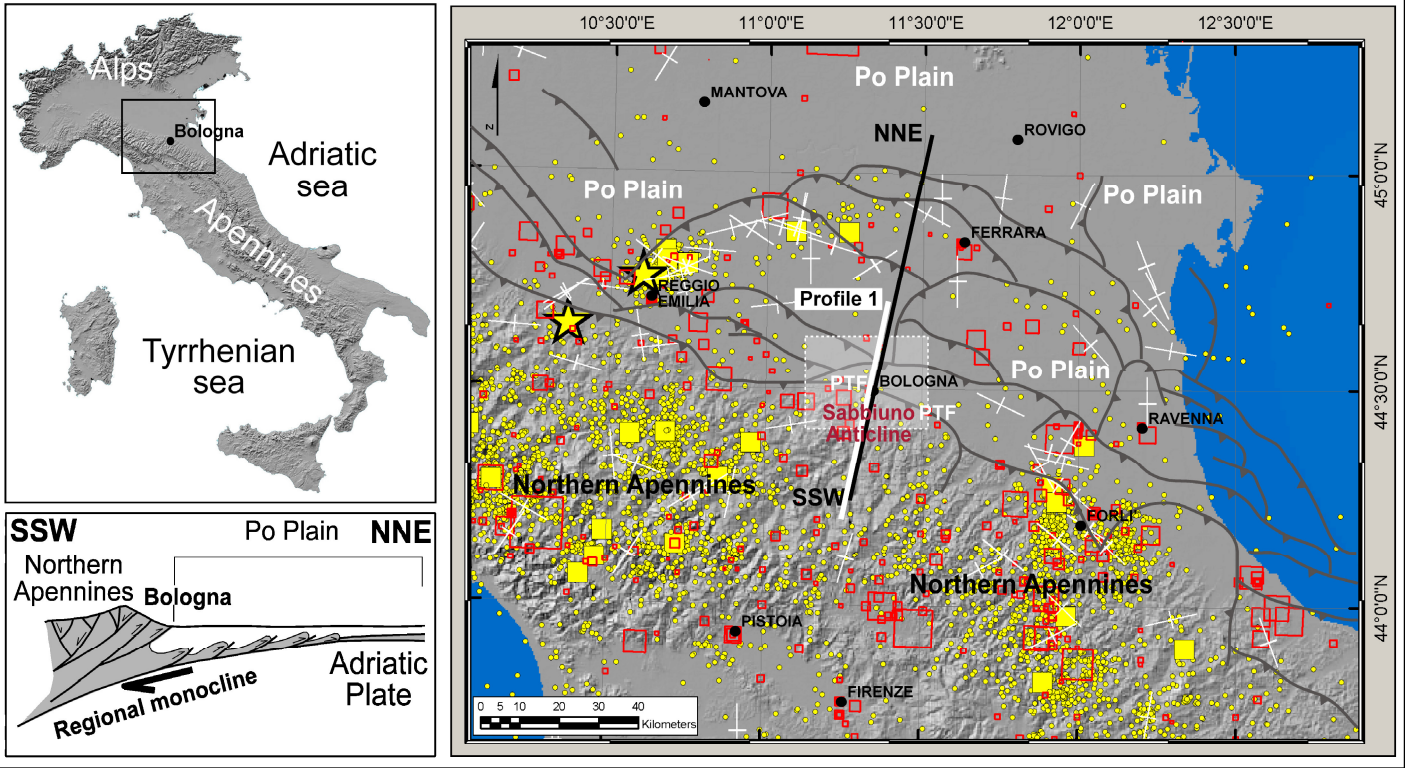


Figure2

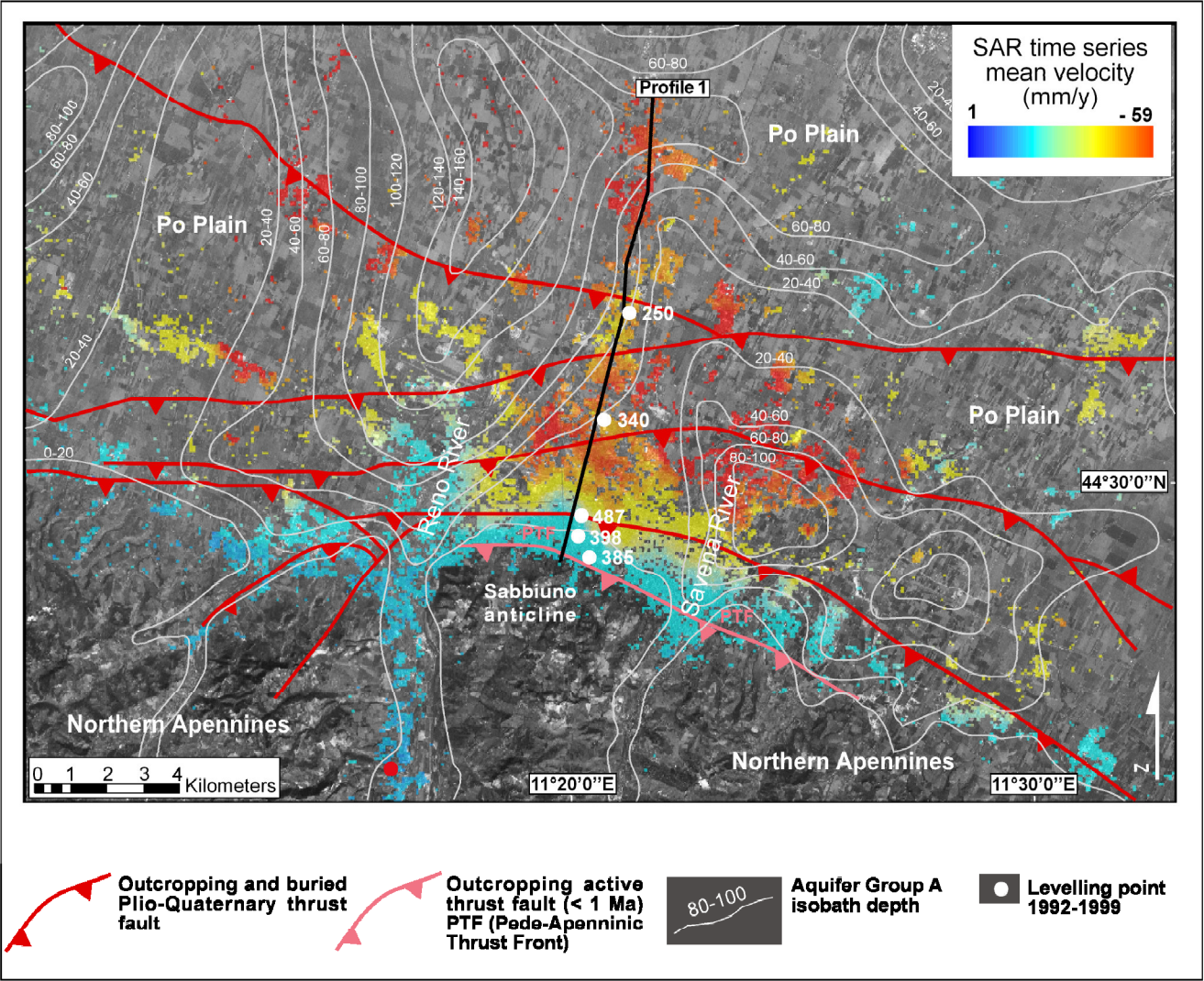


Figure3

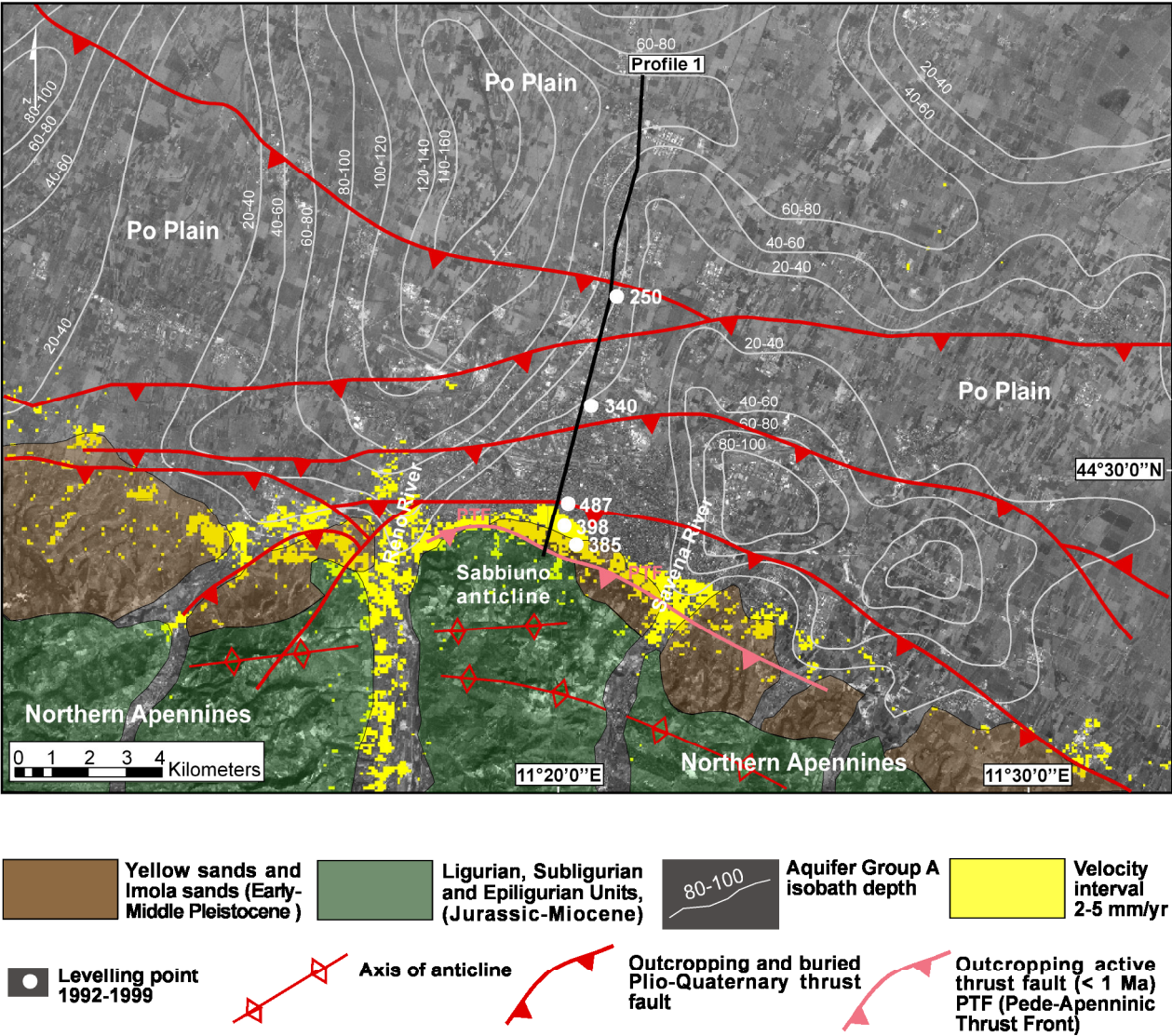


Figure4

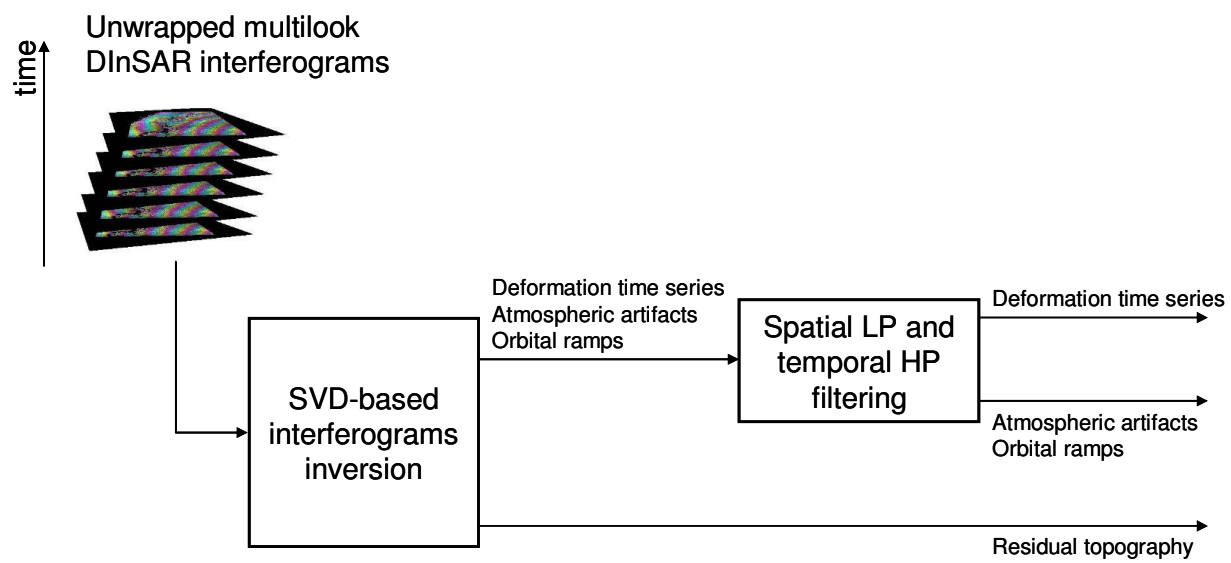


Figure5

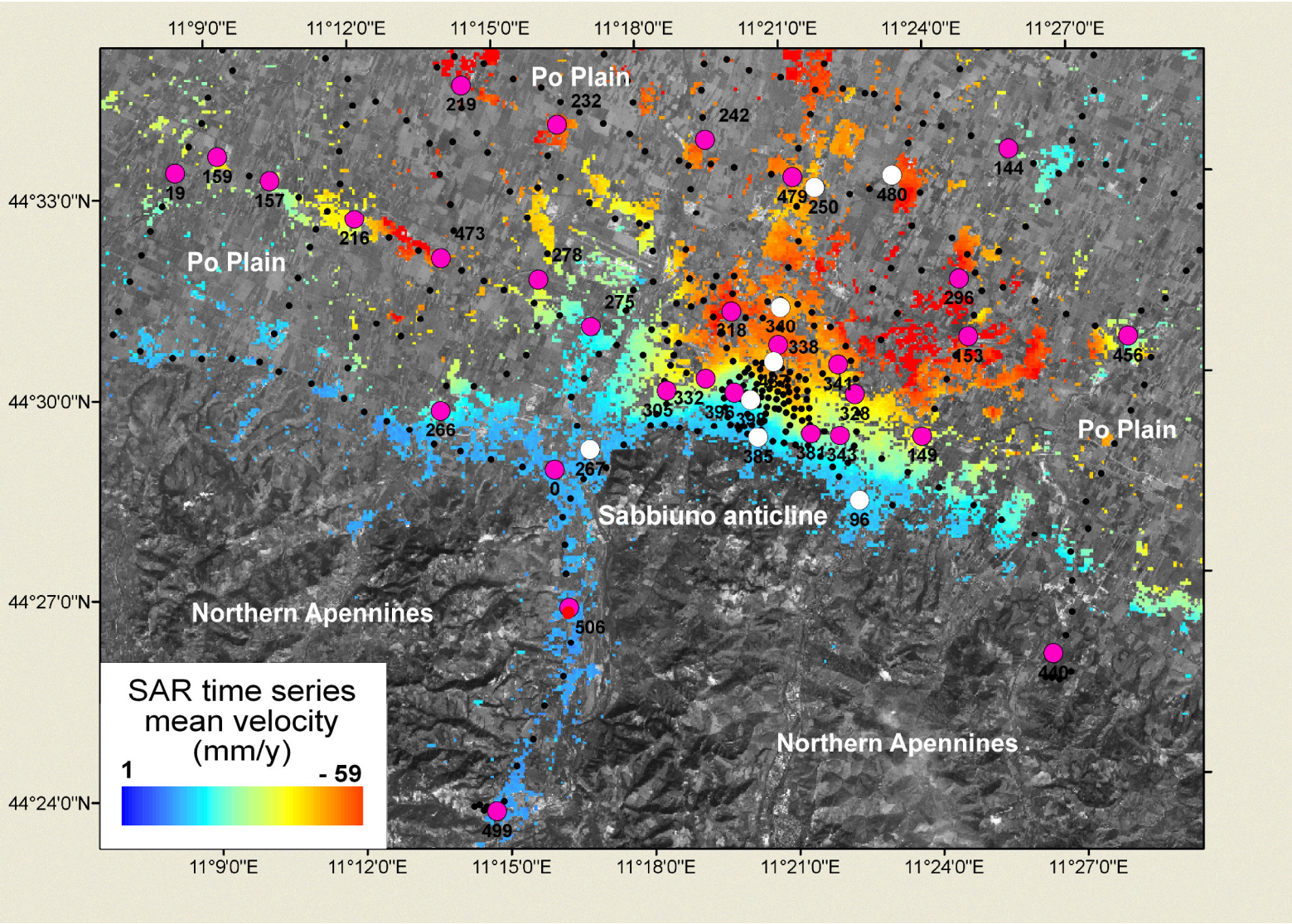
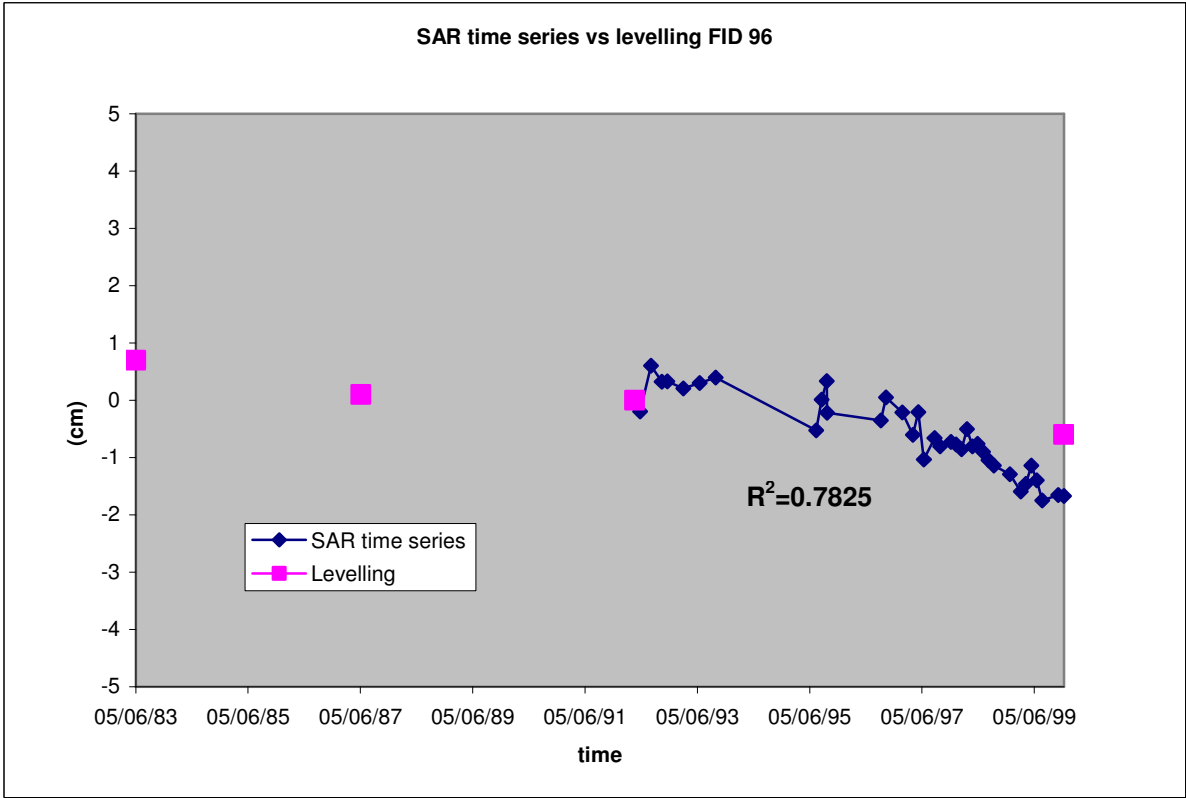
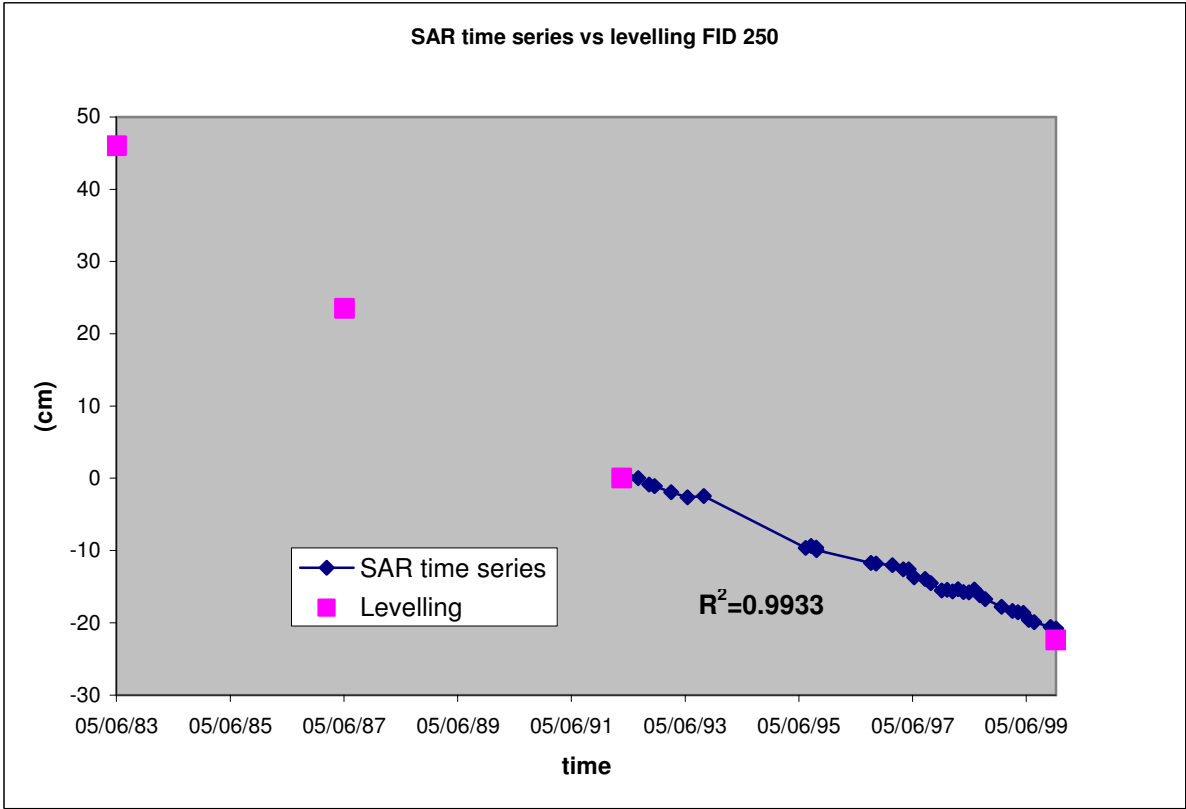


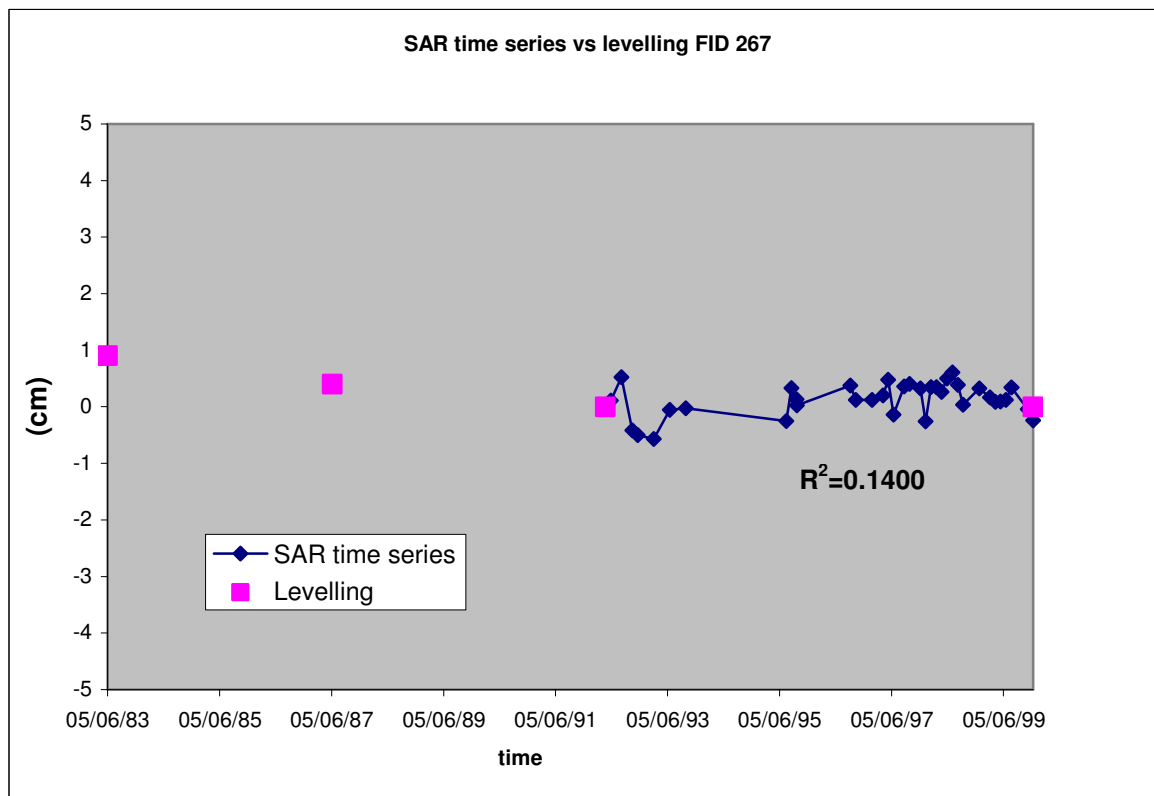
Figure6



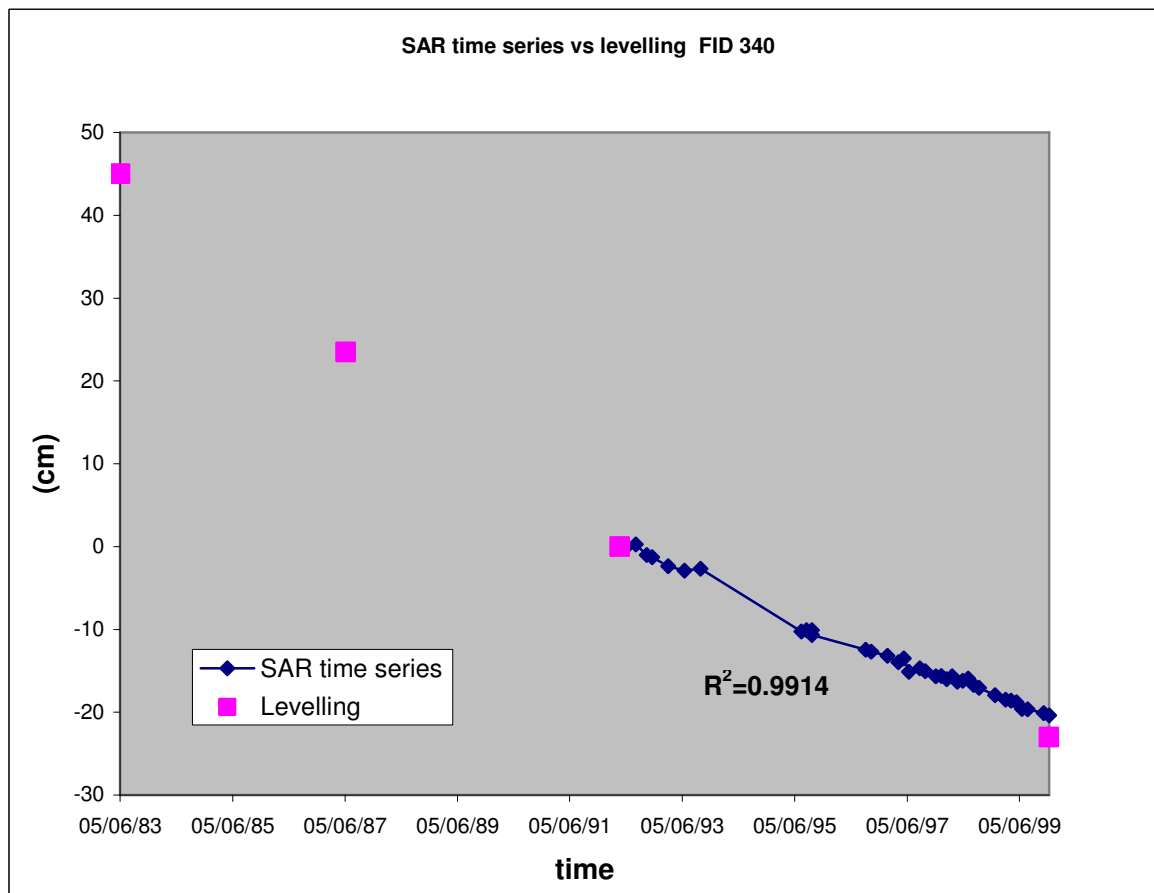
a



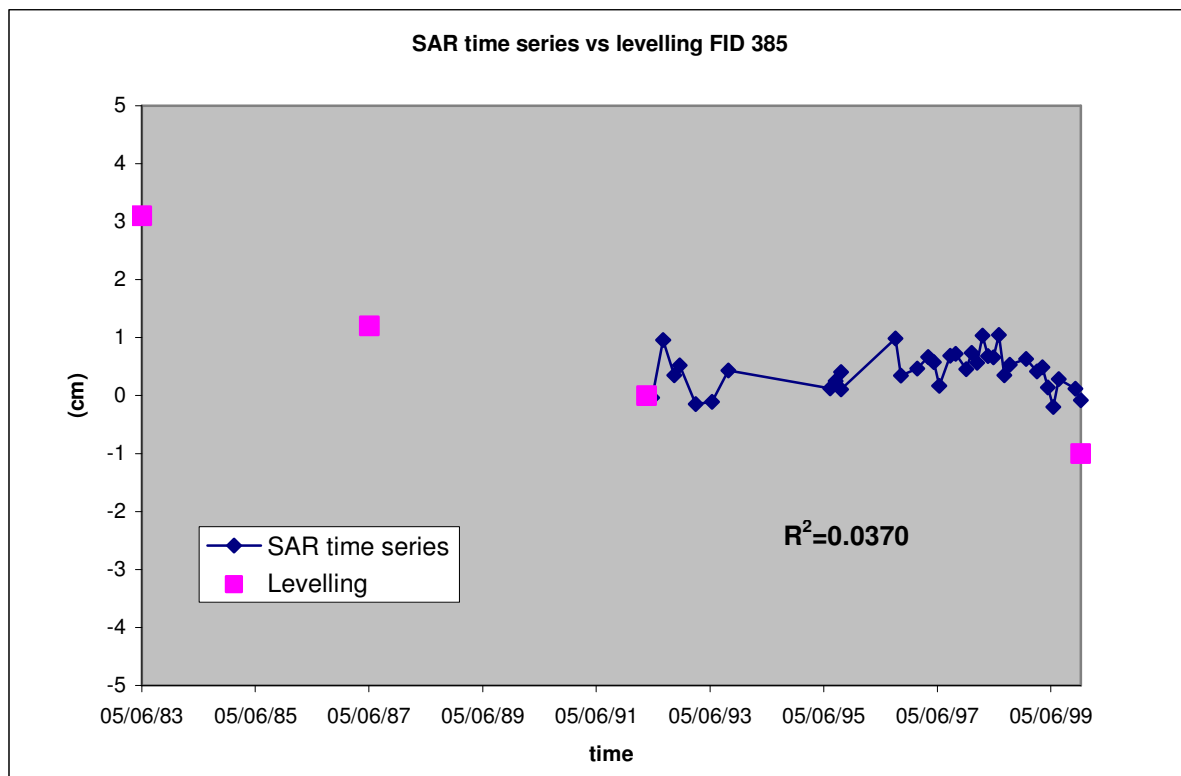
b



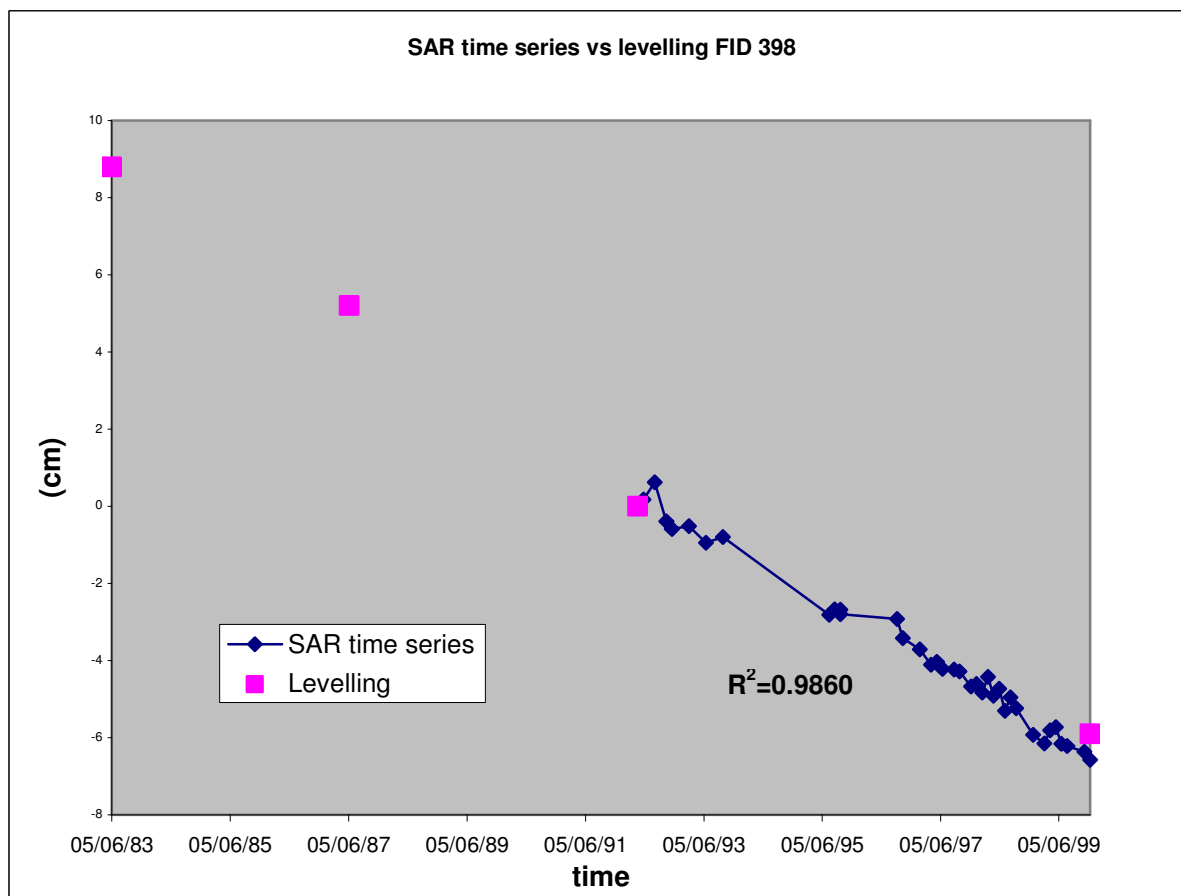
c



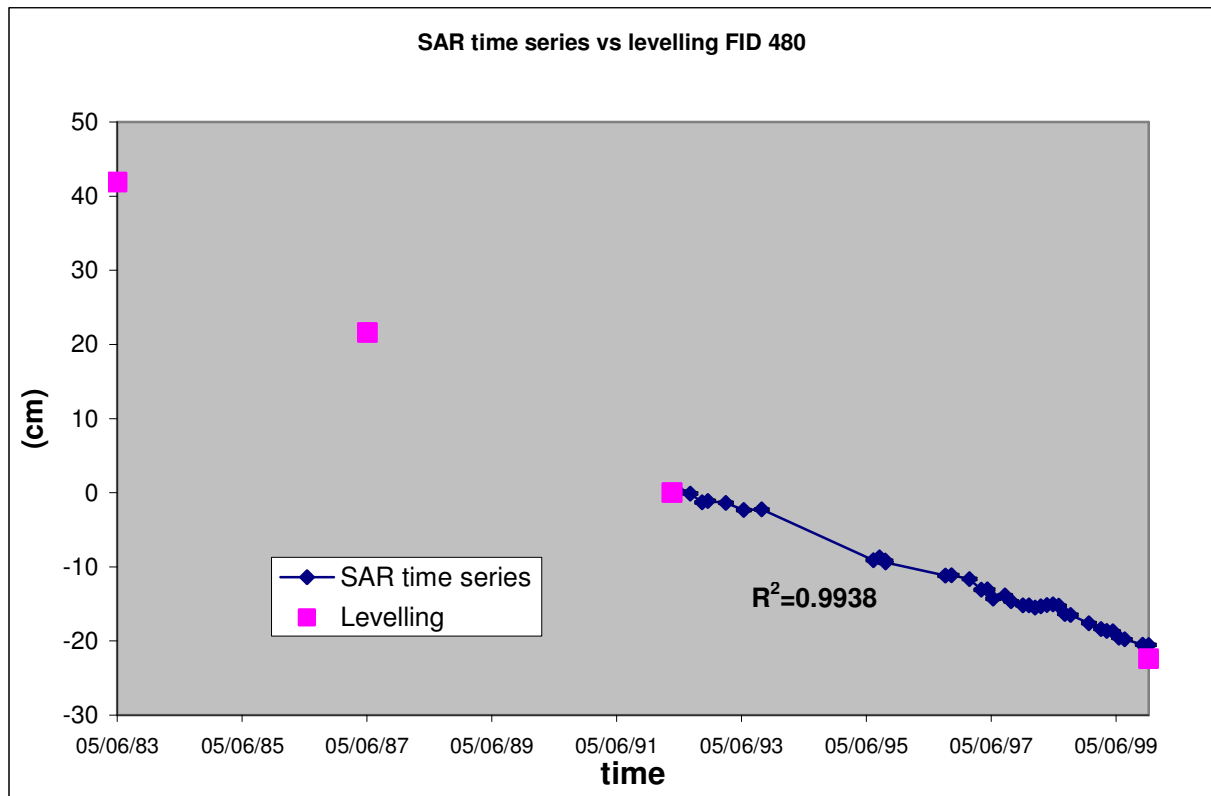
d



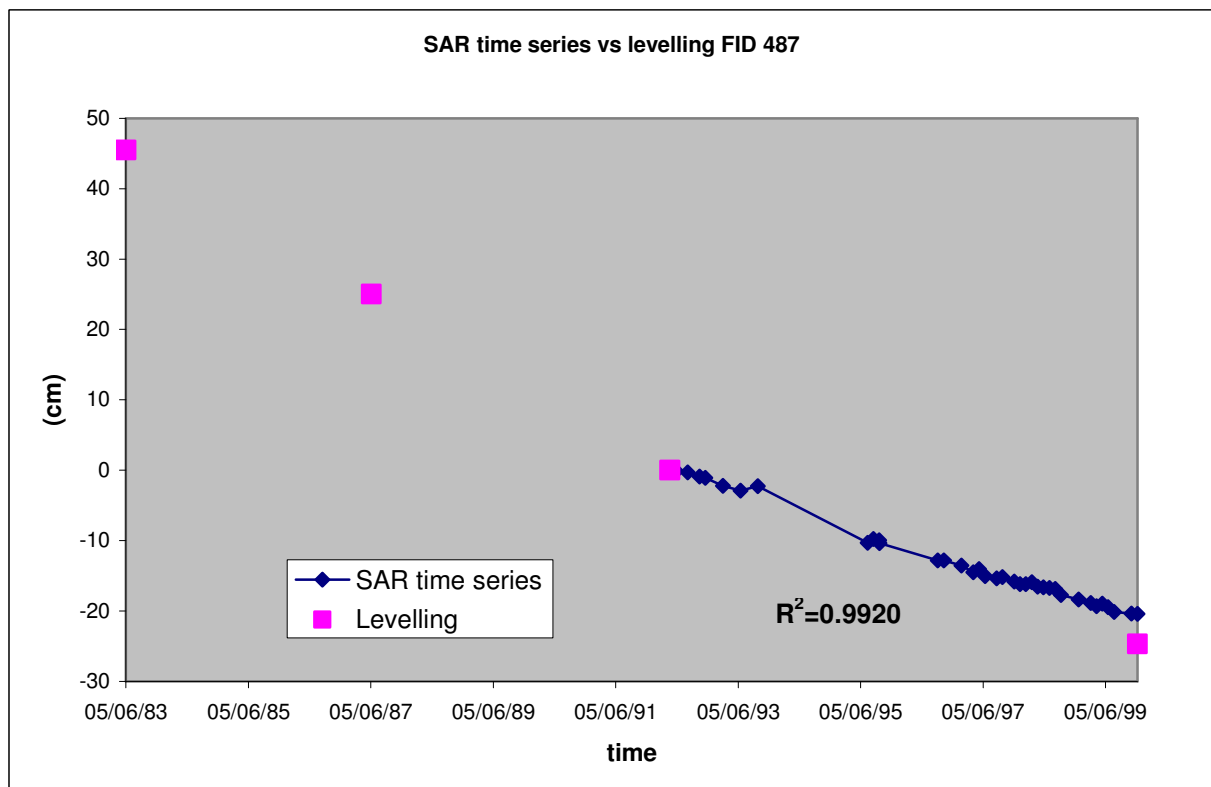
e



f

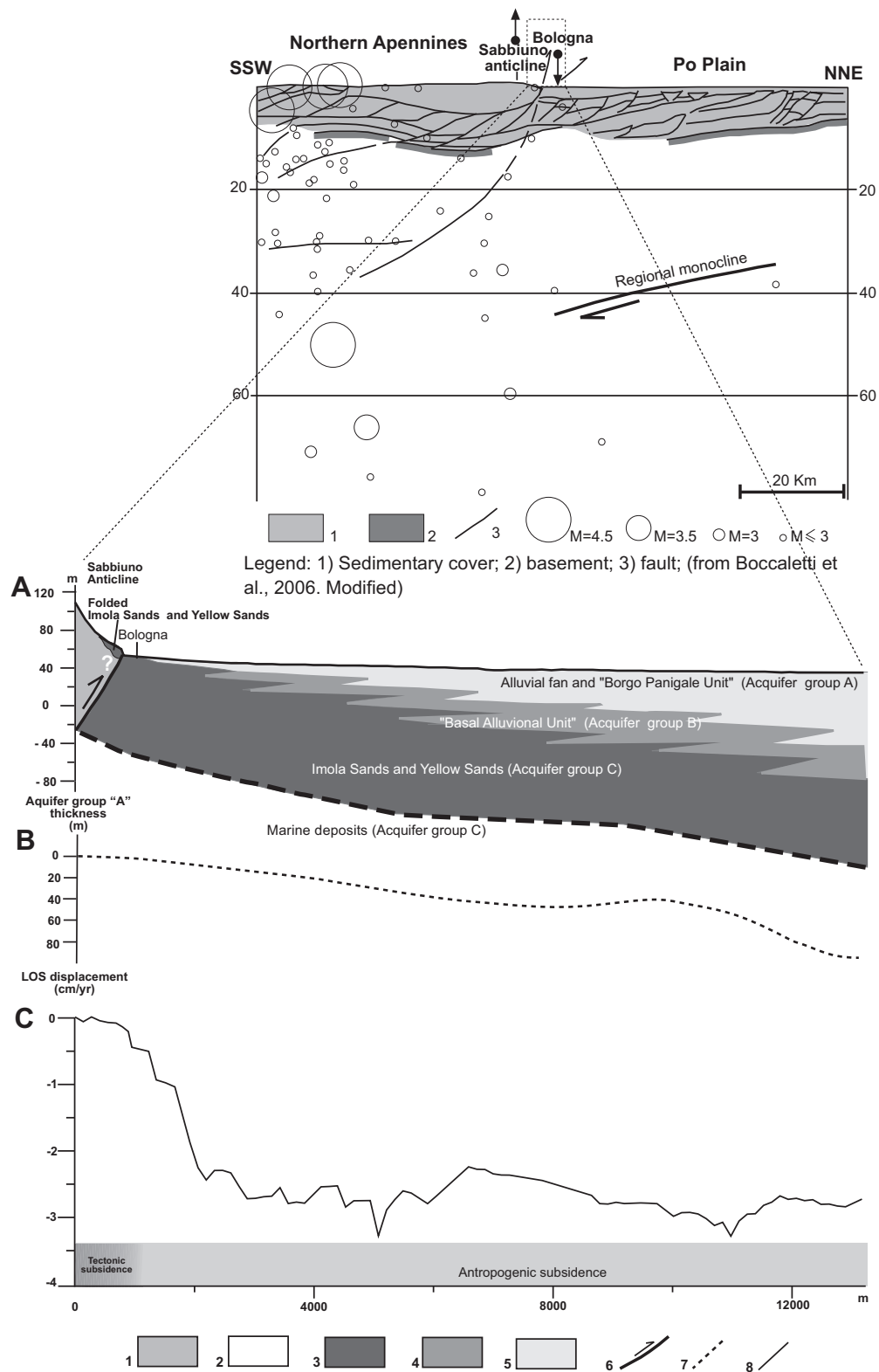


g



h

Figure7



(A) Simplified hydrostratigraphic section (Profile 1 in Fig. 1 and 2). From RER and Eni-Agip, 1998. Modified. Legend: 1) Sabbiuno anticline: Ligurian, Subligurian and Epiligurian Units (Jurassic-Miocene, 205-6,8 My); evaporitic and clastic deposits (Early and Middle Messinian, 6,8-6,3 My); lagoonal and marine deposits (Late Messinian-Early Pliocene, 6,3-4,5 My). 2) Post early Pliocene tectonic phase marine deposits (4,5-1 My): Acquifer group, confined (acquitard). 3) Yellow sands (Early Pleistocene, 1- 0,8 My) and Imola sands (Middle Pleistocene, 0,8-0,65 My): Acquifer group C, confined (acquitard). 4) "Basal Alluvional Unit" (0,65-0,35 My): Acquifer group B, semi-confined. 5) Alluvial fan and "Borgo Panigale Unit" (0,35-0,12 My): Acquifer group A, free-watertable. 6) Active thrust fault (< 1 My). **B)** Legend: 7) Aquifer group "A" thickness (from: RER and Eni-Agip, 1998). **C)** Legend: 8) DInSAR SBAS LOS (Line Of Sight) soil velocity due to both anthropic and natural subsidence.